

ESI

Adaptable Ionic Liquid-Containing Supramolecular Hydrogel with Multiple Sensations at Subzero Temperatures

Bo Li,^a Lei Kan,^a Chao Li,^b Wei Li,^c Yihan Zhang,^a Rui Li,^a Hao Wei,^a Xinyue Zhang*^a
and Ning Ma*^a

^a. Key Laboratory of Superlight Material and Surface Technology of Ministry of Education, College of Material Science and Chemical Engineering, Harbin Engineering University, Nantong Road 145, Harbin, 150001, China.

^b. National ASIC Design Engineering Centre, Institute of Automation, Chinese Academy of Sciences, Beijing, 100190, China

^c. College of Automation, Harbin Engineering University, Nantong Road 145, Harbin, 150001, China.

Corresponding Author

*E-mail: xinyue@hrbeu.edu.cn (X. Zhang)

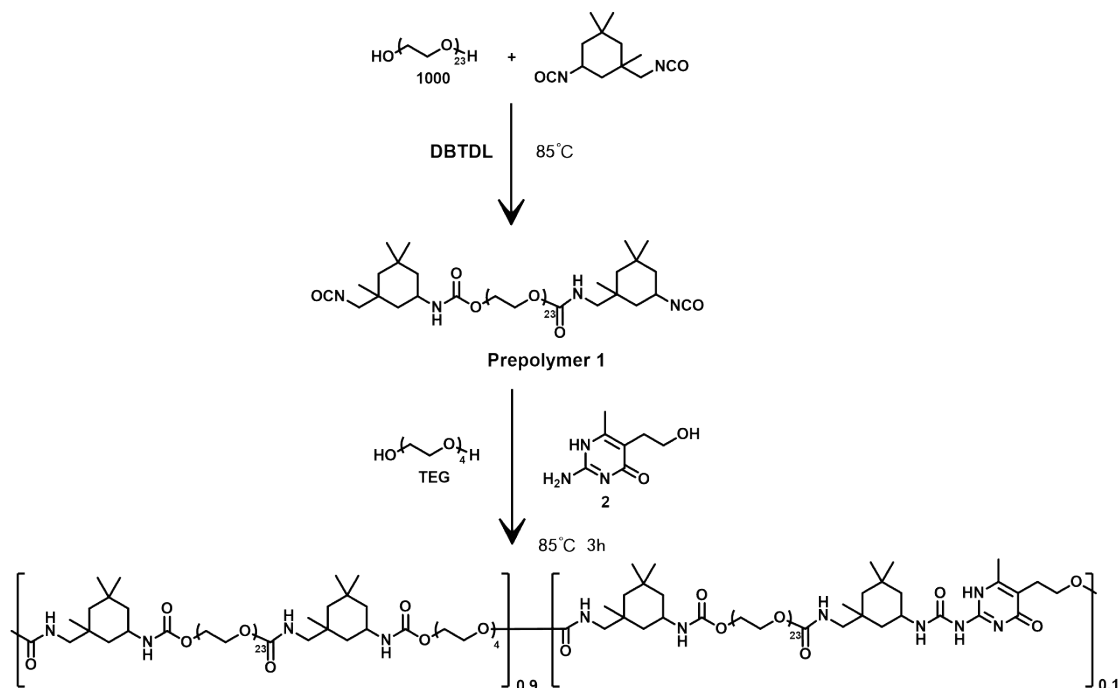
*E-mail: nma@hrbeu.edu.cn (N. Ma)

Contents

1. The main synthetic process of supramolecular polymer and formation of SPIH. (Fig. S1)
2. The general characterizations of SPIH. (Fig. S2-3)
3. The viscoelastic tests of supramolecular and ionic liquid hydrogels. (Fig. S4-5)
4. The responsive testing of SPIH. (Fig. S6-7)
5. The application testing of SPIH. (Fig. S8-9)
6. The SPIH containing diverse ions or particles performance versatility. (Fig. S10)

1. The main synthetic process of supramolecular polymer and formation of SPIH.

a)



b)

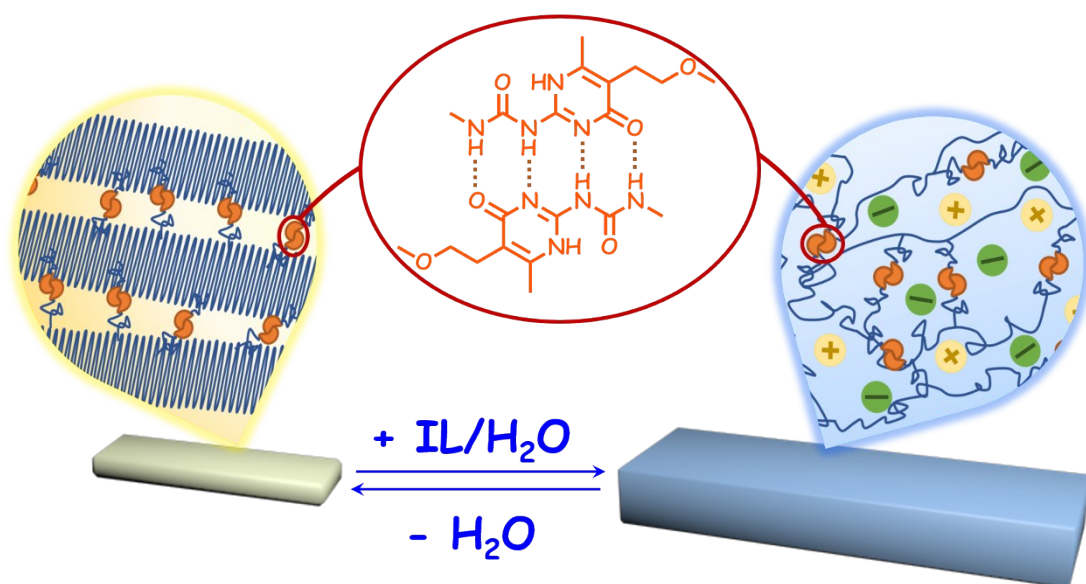


Fig. S1 a) The synthetic process. b) Cartoon representation of the formation and proposed mechanism for highly stretchable SPIH.

2. The general characterizations of SPIH.

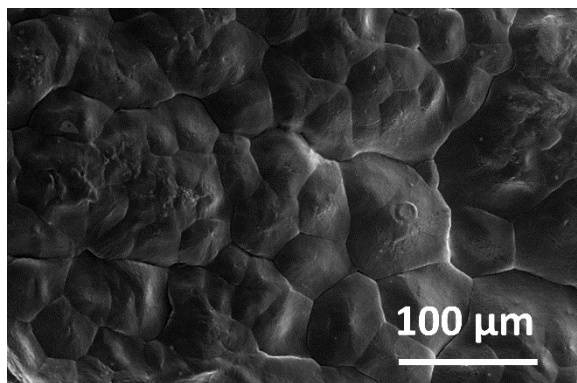


Fig. S2 The SEM image of the freeze-dried SP6IH, which showed wrinkles on the surface due to the shrinkage at the dehydration process.

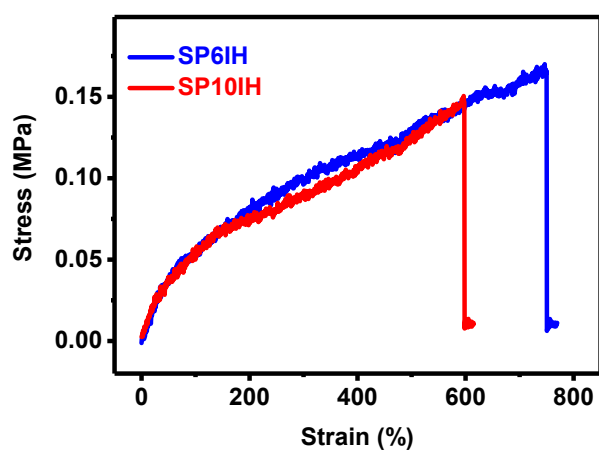


Fig. S3 The static tension tests of the two SPIHs with different ionic liquids.

3. The viscoelastic tests of supramolecular and ionic liquid hydrogels.

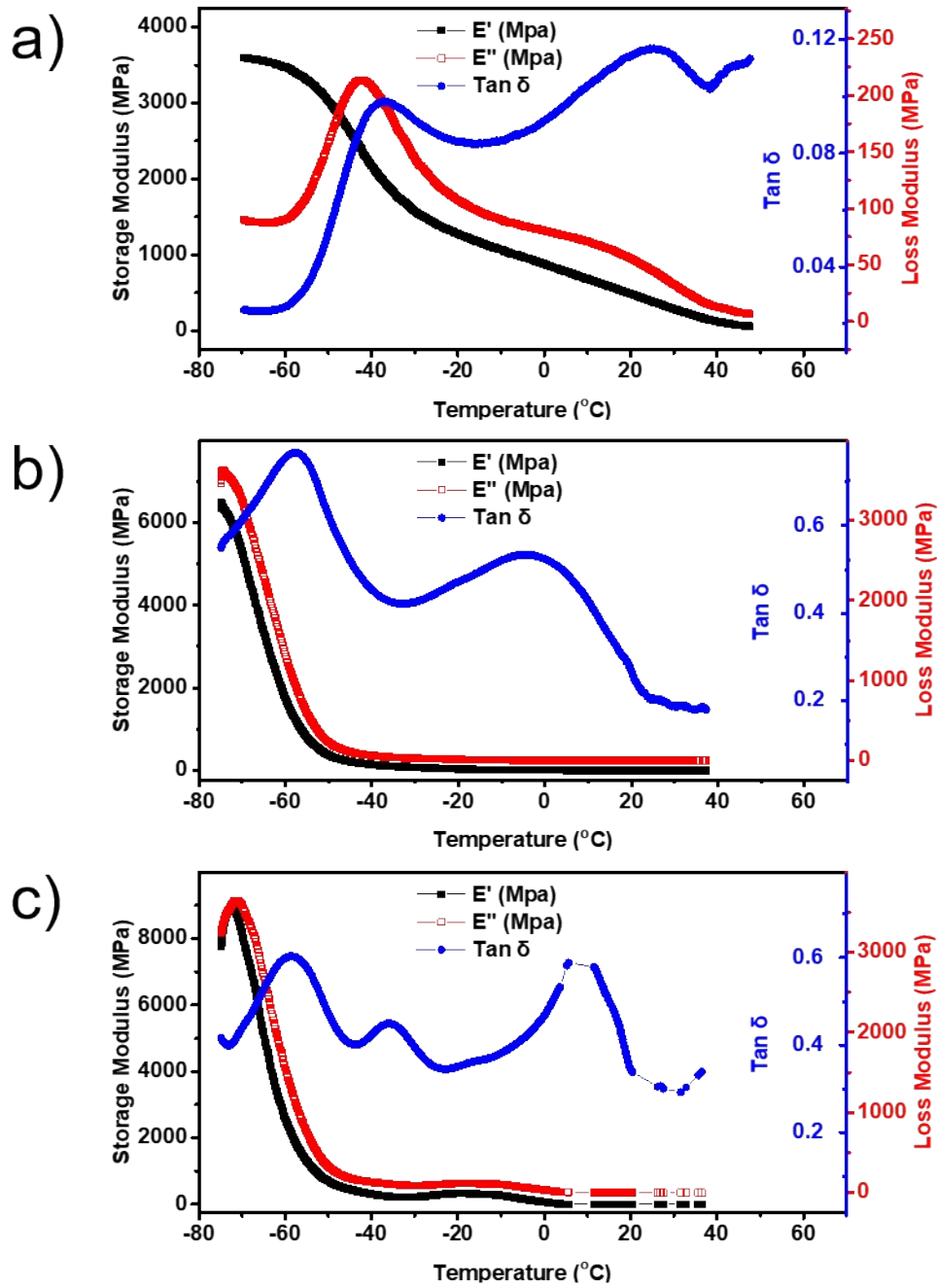


Fig. S4 The DMA curves of a) SP, b) SP6IH c) SP10IH.

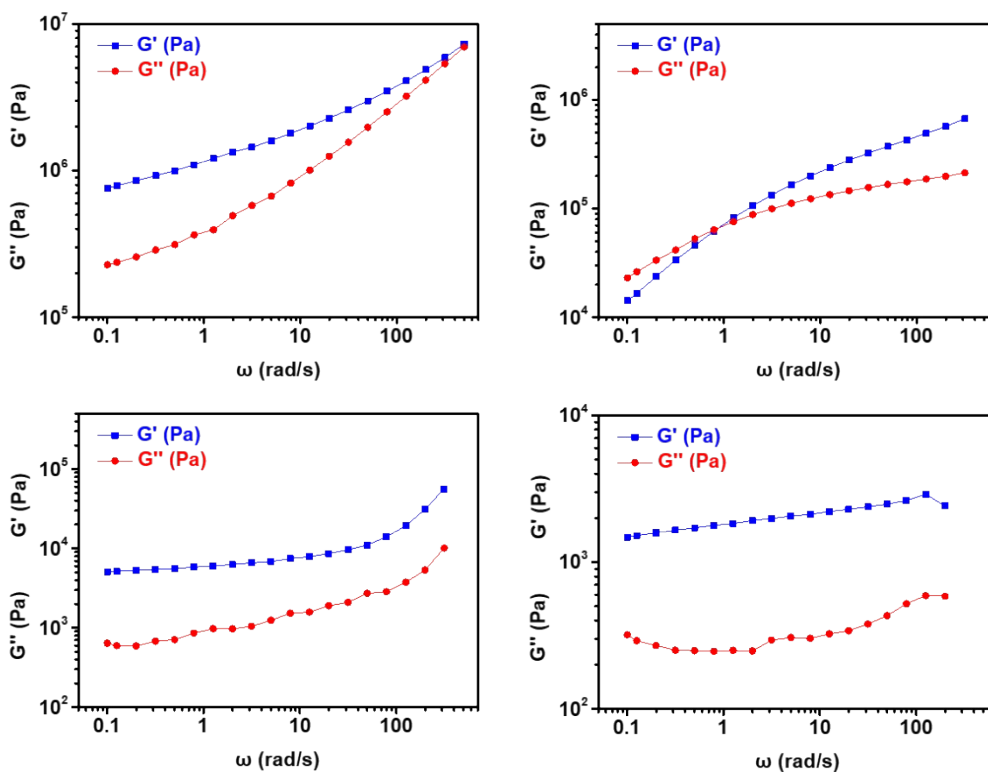


Fig. S5 The rheology tests of supramolecular and ionic liquid hydrogels SP10IL. The oscillatory frequency rheology tests of SP at a) -20°C and b) 40°C 0.1% strain. The oscillatory frequency rheology tests of c) SP6IH and d) SP10IH at 40°C , 0.1% strain.

4. The responsive testing of SPIH.

As a contrast, the thermal response of SP10IH was also studied below.

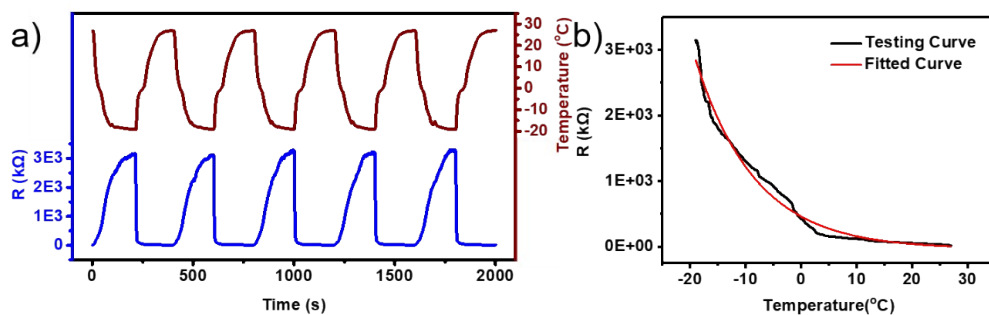


Fig. S6 The temperature-responsive testing of SP10IH. a) The resistance changing curves versus temperature from $-20 - 25^{\circ}\text{C}$. b) The resistance curve fitted the Vogel-Tammann-Fulcher (VTF) equation basically from $-20 - 25^{\circ}\text{C}$.

To certify the stability of SP6IH film, 500 tensile-relaxation cycles had been carried out.

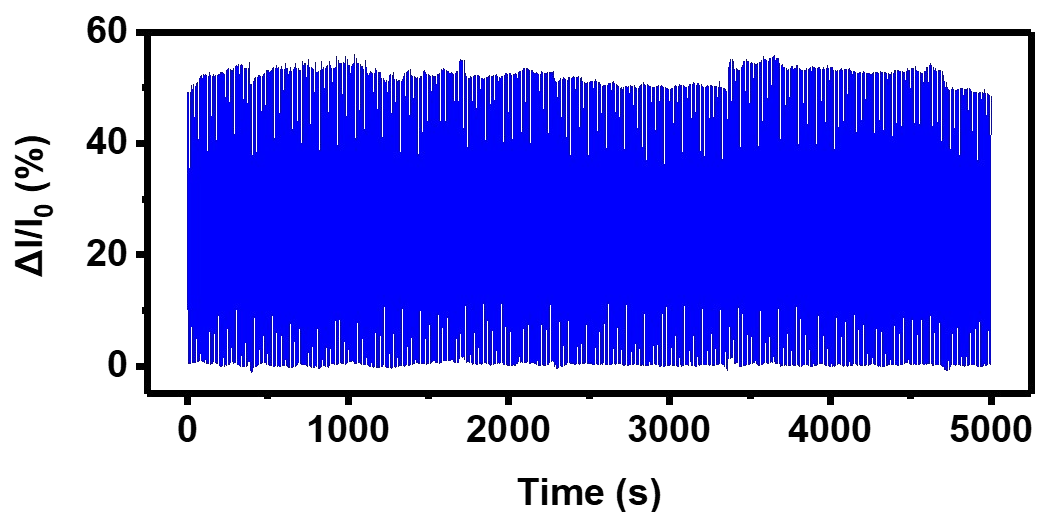


Fig. S7 The tension-responsive testing of SP6IH for 500 cycles.

5. The application testing of SPIH.

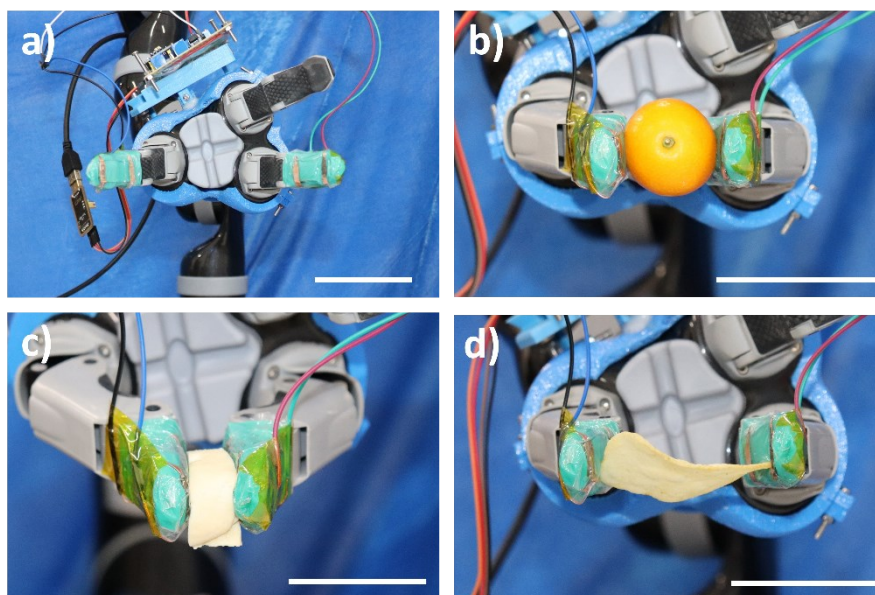


Fig. S8 The manipulator clamp experiments with SP6IH as the pressure sensitive flexible artificial E-skin sensor (KINOVA Gen3 Ultra lightweight robot). a) The SP6IH film was attached on the inner side of the manipulator finger and to touch and grab b) kumquat, c) Chinese tofu, d) potato chip. (Scale bar: 5 cm)

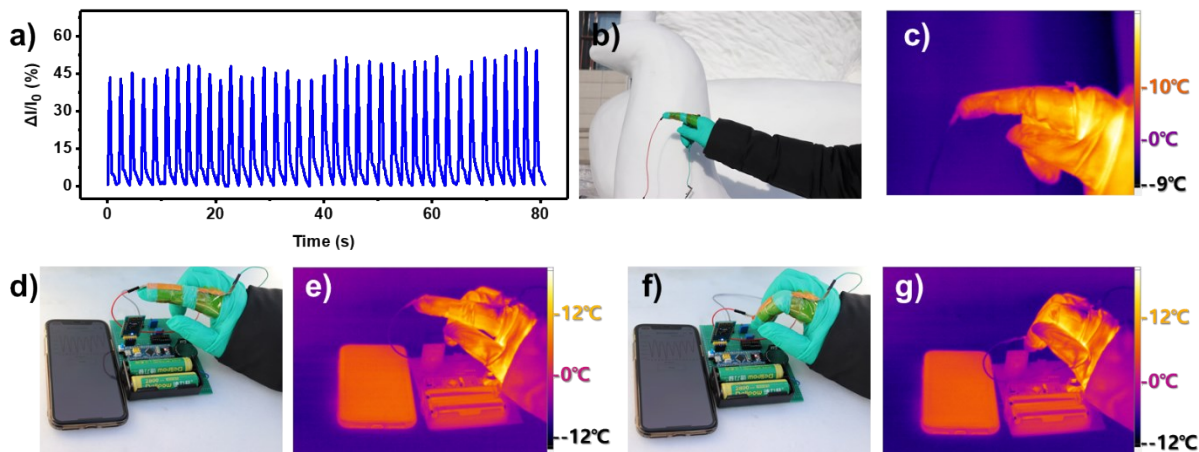


Fig. S9 The motion monitoring performance of SP6IH sensor in winter outdoors. a) The current changes with cyclic bending motion detection of finger. The sensor was stuck on the finger joint and bended for several times. b) The optical image and c) IR thermal image of the bending tests. d), f) The optical image and e),g) IR thermal image of the real-time motion detection monitoring through Bluetooth devices.

In order to expand the application of SPIH, different functional dispersions were contained by SPIH.

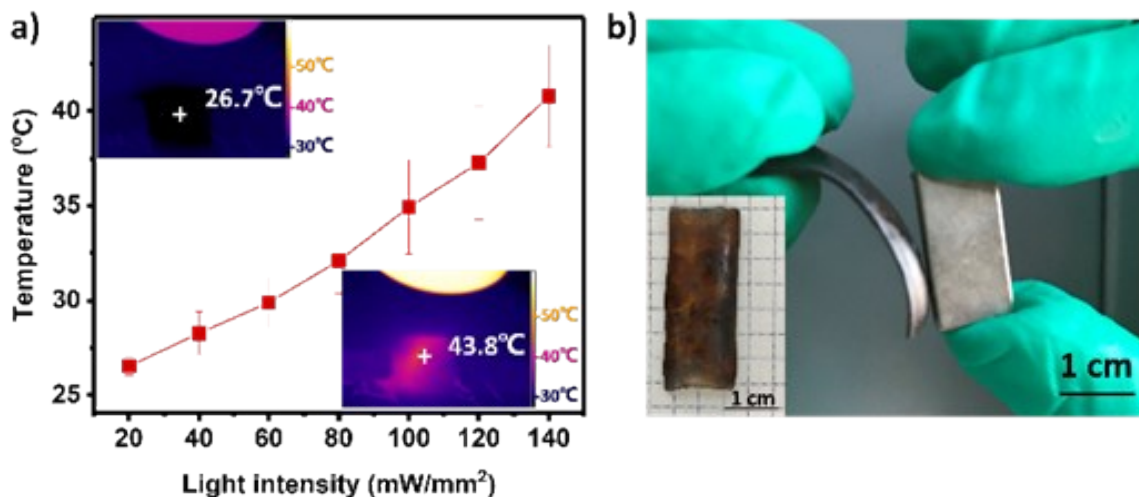


Fig. S10 The SPIH containing diverse ions or particles performance versatility. (a) The SPIH containing CuSO_4 possessed photo-thermal conversion property under 808 nm near-infrared light. The inner IR thermal images in the upper left showed SPIH under 20 mW/mm^2 NIR irradiated for 100 s and the one in the right corner under 140 mW/mm^2 . (b) The SPIH swelling with Fe_3O_4 nano particles dispersion could be magnet attracted.